ACS APPLIED MATERIALS & INTERFACES

Research Article

www.acsami.org

Novel Anisotropic Magnetoelectric Effect on δ-FeO(OH)/P(VDF-TrFE) Multiferroic Composites

P. Martins,[†] A. Larrea,[‡] R. Gonçalves,[†,§] G. Botelho,[§] E. V. Ramana,[∥] S. K. Mendiratta,[∥] V. Sebastian,[‡,⊥] and S. Lanceros-Mendez*[,†]

[†]Centro/Departamento de Física, Universidade do Minho, 4710-057 Braga, Portugal

[‡]Department of Chemical Engineering. Aragon Institute of Nanoscience (INA), University of Zaragoza, Campus Río Ebro-Edificio I+D, C/Poeta Mariano Esquillor S/N, 50018 Zaragoza, Spain

[§]Centro/Departamento de Química, Universidade do Minho, 4710-057 Braga, Portugal

[∥]Departamento de Física, Universidade de Aveiro, Campus Universitário de Santiago, 3810-193 Aveiro, Portugal

[⊥]CIBER de Bioingeniería, Biomateriales y Nanomedicina (CIBER-BBN), C/Monforte de Lemos 3-5, Pabellón 11, 28029 Madrid, Spain

ABSTRACT: The past decade has witnessed increased research effort on multiphase magnetoelectric (ME) composites. In this scope, this paper presents the application of novel materials for the development of anisotropic magnetoelectric sensors based on δ-FeO(OH)/P(VDF-TrFE) composites. The composite is able to precisely determine the amplitude and direction of the magnetic field. A new ME effect is reported in this study, as it emerges from the magnetic rotation of the δ-FeO(OH) nanosheets inside the piezoelectric P(VDF-TrFE) polymer matrix. δ-FeO(OH)/P(VDF-TrFE) composites with 1, 5, 10, and 20 δ-FeO(OH) filler weight percentage in three δ-FeO(OH) alignment states (random, transversal, and longitudinal) have been developed. Results have shown that the modulus of the piezoelectric response (10−24 pC·N^{-1}) is stable at least up to three months, the shape and magnetization maximum value (3 emu·g^{-1}) is dependent on δ-FeO(OH) content, and the obtained ME voltage coefficient, with a maximum of ∼0.4 mV·cm^{-1}·Oe^{-1}, is dependent on the incident magnetic field direction and intensity. In this way, the produced materials are suitable for innovative anisotropic sensor and actuator applications.

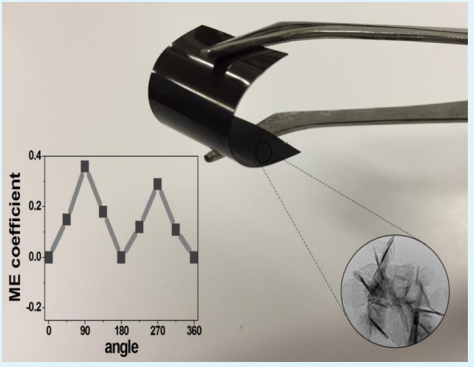

KEYWORDS: *magnetoelectrics, anisotropic, polymer-based, sensors, multiferroic*

INTRODUCTION

The magnetoelectric (ME) effect is characterized by the variation of the electrical polarization of a material in the presence of an applied magnetic field.[1−3] The opposite phenomenon is also observed, i.e., a magnetization variation is induced by applying an electric field. The effect can occur intrinsically or extrinsically, mediated by the elastic coupling between the magnetostrictive and the piezoelectric components.[4,5]

Single-phase materials (intrinsic ME effect) are not very interesting from the point of view of applications because they have commonly weak ME coupling at room temperatures.[6] To avoid such a problem, a strong ME effect at room temperature has been obtained in ME composites, in particular in those composed by a piezoelectric and a magnetostrictive phase.[4] In such materials, a strain is induced on the magnetostrictive phase once a magnetic field is applied to the composite.[7] This strain is transmitted to the piezoelectric constituent, which undergoes a change in the electrical polarization.[8] In an analogous way, the reverse effect can occur: when an electric field is applied to the composite, strain is induced in the piezoelectric phase, which is transmitted to the magnetostrictive phase, leading to a change in the magnetization.[4]

Actuators, magnetic memories, multifunctional sensors, resonators, microwave and energy harvesting devices are the main applications of ME materials.[9,10] One of the main applications of ME materials is nevertheless in the area of novel magnetic sensors.[4,7] When compared to other types of sensors including search coils fluxgate, optical pumps, superconducting quantum interference device, Hall-effect, magnetoresistance or giant magneto-impedance magnetic sensors,[4,7] ME sensors offer unique and valuable characteristics such as low-cost materials and fabrication, room-temperature response, low size, self-powered and noncontact sensing, high sensing resolution (pT), large dynamic range, good time stability, the possibility of a flat frequency response, and reduction of the equivalent magnetic noise.[4,7,11]

Received: February 6, 2015
Accepted: May 7, 2015
Published: May 7, 2015

DOI: 10.1021/acsami.5b01196
ACS Appl. Mater. Interfaces 2015, 7, 11224−11229

Such ME composites used as magnetic sensors can be ceramic-based or polymer-based.[12] Polymer-based ME materials have some advantages when compared to ceramic ones due to their flexibility and the fact that they can be easily fabricated by conventional low-temperature processing into a variety of forms, such as thin sheets or molded shapes, with improved mechanical properties.[13] Three main types of ME polymer-based composites can be found: *polymer as a binder*, laminates, and particulate nanocomposites.[4] All of them take advantage of the good coupling between the magnetostrictive and piezoelectric materials.

ME coefficients, ranging from 1 to 400 000 $mV \cdot cm^{-1} \cdot Oe^{-1}$, obtained on polymer-based ME nanocomposites allow the fabrication of magnetic sensors with enormous potential for other byproducts related to them: electric current sensors, speed sensors, angular sensors, electronic steering, throttle control, battery management, vehicle transmission, digital compasses, and GPS devices.[4,14] Additionally it has been reported that the ME magnetic sensors exhibit larger application prospects in geomagnetic field measurements when compared to traditional magnetic sensors such as magnetoresistant sensors or fluxgate sensors.[15−17] In general, high ME anisotropy is critically necessary for ME single-axis sensors, which are capable of probing the magnitude as well as the direction of the magnetic field vector.[16] This new concept of anisotropic ME magnetic sensors, despite having high interest in applications such as navigation, motion tracking, sports, and healthcare, remains vaguely explored,[16,18−20] with it being not possible to find in literature reports on anisotropic magnetic sensors built on ME polymer-based materials.

In the present work, the anisotropy of the ME response[21] is obtained by the introduction of magnetic nanosheets of feroxyhyte (δ-FeO(OH)) in a poly[vinylidenefluoride-*co*-trifluoroethylene] (P(VDF-TrFE)) piezoelectric matrix. The ME effect on the δ-FeO(OH)/P(VDF-TrFE) composites will not arise in the traditional way, by the coupling between the magnetostriction and piezoelectricity, but instead by the alignment of the feroxyhyte nanosheets, as a response to the applied magnetic field, on the P(VDF-TrFE) matrix.

P(VDF-TrFE) was used as the piezoelectric phase because it has one of the highest piezoelectric response among a small class of polymers that exhibit piezoelectricity. Additionally, when crystallized from the melt, this PVDF copolymer crystallizes in the piezoelectric phase (being also ferroelectric), which is an essential factor for the preparation of ME composites.[4,14]

Feroxyhyte nanosheets were chosen as the magnetic component because of their simple preparation method, anisotropic magnetic response, and absence of magnetostrictive properties as, in this way, the ME response emerges from the rotation of the nanosheets and not from the magnetostriction.[16] As a result, the development of δ-FeO(OH)/P(VDF-TrFE) composites with anisotropic ME response, able to detect the magnetic field amplitude and direction, is reported.

EXPERIMENTAL SECTION

(a). Nanoparticle Synthesis. The δ-FeO(OH) nanosheets were synthesized using a polytetrafluoroethylene (PTFE) microfluidic reactor by a liquid−gas segmented flow. Inlet flow A, composed of an aqueous solution of 180 mM KNO_3, 162 mM NaOH, and 1.85 mM L-lysine, was mixed with an inlet flow B, which consisted of an aqueous solution of 13 mM ferrous sulfate heptahydrate (with Fe^{2+} cations) and 3.38 mM sulfuric acid (Figure 1).

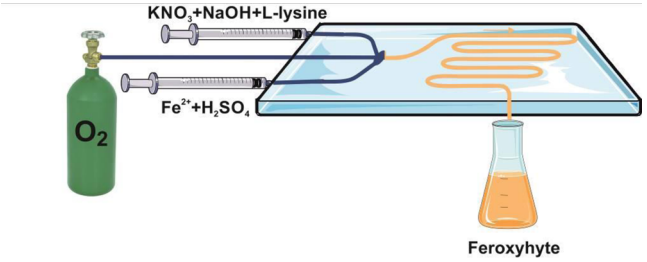

Figure 1. Schematic representation of the synthesis process of the feroxyhyte nanosheets.

Inlet flows A and B were injected in a Y junction with an O_2 flow at the proper flow rate to achieve a steady segmented flow. The compartmentalized slugs were heated at 90 °C, obtaining at the microreactor outlet an orange solution that was identified with a pure feroxhyte phase. Afterward, the synthesized nanoparticles were centrifuged at 10.000 rpm for 10 min, then washed twice with distilled water, and finally resuspended in distilled water for further use.

(b). Composite Preparation. The desired amount of the magnetic phase (Figure 2a) was added to *N*,*N*-dimethylformamide

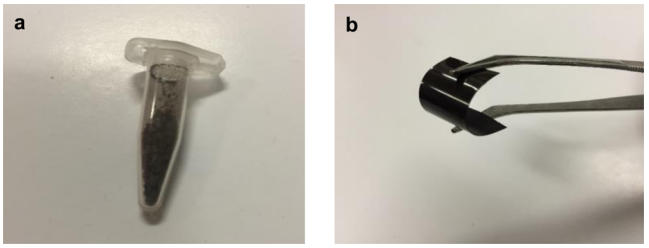

Figure 2. (a) Obtained feroxhyte nanosheets. (b) Flexible multiferroic δ-FeO(OH)/P(VDF-TrFE) composite films.

(DMF, pure grade, supplied by Fluka) and placed in an ultrasound bath for 8 h in order to ensure a good dispersion of the nanosheets. Flexible ME composite films were prepared (Figure 2b), with 1, 5, 10, and 20 δ-FeO(OH) filler weight content (wt %); P(VDF-TrFE) polymer (supplied by Solvay Solexis) was then added and mixed during 2 h with the help of a mechanical Teflon stirrer in an ultrasound bath to avoid the magnetic agglomeration during the mixing process. After that, the solution was spread in a clean glass substrate, and solvent evaporation and samples crystallization took place at 80 °C while it was placed between the two coils of an electromagnet to ensure the magnetic alignment along the length direction (longitudinal-L samples, Figure 3a) and along the thickness direction (transversal-T samples, Figure 3b) of the composite film of the δ-FeO(OH) nanosheets. A sample with random δ-FeO(OH) filler orientation was also prepared (A samples, Figure 3c).

During the alignment process, solvent evaporation occurred at 80 °C in order to obtain flexible films, without pores and with good mechanical properties (Figure 2b).[22] Polymer crystallization ended by

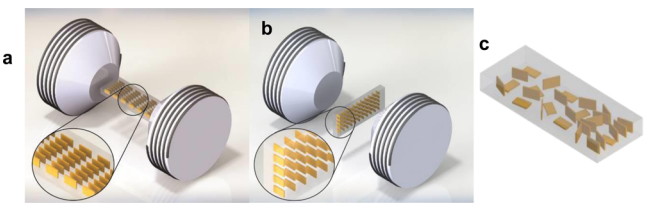

Figure 3. Representation of (a) magnetic alignment along the length direction; (b) magnetic alignment along the thickness direction; (c) randomly oriented samples.

DOI: 10.1021/acsami.5b01196
ACS Appl. Mater. Interfaces 2015, 7, 11224−11229

cooling down films to room temperature. At the end of the process, the flexible film was peeled from the glass substrate and a film with an average thickness of ~25 μm was obtained.

(c). Sample Characterization. The magnetic properties of the nanoparticles were measured as dried powders after solvent evaporation at different temperatures in a superconducting quantum interference device (SQUID MPMS-5S, Quantum Design) from 0 to 40 000 Oe. The samples were measured in a gelatin capsule (a diamagnetic correction for the sample holder was carried out). Magnetic hysteresis loops (magnetization of the sample as a function of the magnetic field strength) were evaluated at 37 °C.

The phases of iron oxide nanoparticles were identified by powder X-ray diffraction. The X-ray patterns were collected between 20° and 80° (2θ) in a D-Max Rigaku diffractometer with Cu Kα radiation. The particle morphology and size distribution were determined by transmission electron microscopy (TEM FEI-TECAI T20) operated at 200 kV.

The morphology of composites was studied by scanning electron microscopy (SEM) using a Quanta 650 FEI electron microscope with acceleration voltage of 10 kV. Prior to SEM, the samples were coated with gold by magnetron sputtering. Images were taken in three different locations of the samples and at different magnifications to ensure reproducibility of the observed morphological features.

The piezoelectric response (d_{33}) of the samples was analyzed with a wide range d_{33}-meter (model 8000, APC Int Ltd.) after poling the ME composites by corona poling at 10 kV during 120 min at 120 °C in a homemade chamber and cooling down to room temperature under applied field after an optimization procedure.[23] To obtain the out-of-plane ME coefficient α_{33}, the first index indicating the collinear ferroelectric poling and electrical measurement directions, and the second indicating the applied magnetic field direction, dc and ac magnetic fields were applied along the length of the sample, i.e., in the same direction of the alignment of the nanosheets.

An ac driving magnetic field of 1 Oe amplitude at 7 kHz (resonance of the composite) was provided by a pair of Helmholtz coils and controlled by a signal generator. Such resonance was determined by eq 1,[24,25]

$$f_n \approx (n/2l)\sqrt{E_Y/\rho} \tag{1}$$

where l is the length along the resonant direction, n is the order of the harmonic mode, and ρ and E_Y are density and Young's modulus, respectively.

A dc field with a maximum value of 0.5 T was applied by an electromagnet driven by a dc source. The induced ME voltage was measured with a Standford Research Lock-in amplifier (SR530). The magnetic field direction response on the ME response was studied by rotating the samples (0−360°, Figure 4).

Prior to the ME measurements, δ-FeO(OH)/P(VDF-TrFE) composites were coated by thermal evaporation with 5 mm diameter circular Au electrodes onto both sides of the samples. Three samples

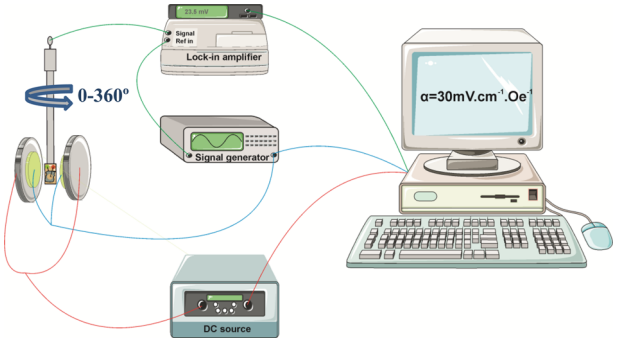

Figure 4. Schematic representation of the experimental setup used to study the influence of the magnetic field direction on the ME response of δ-FeO(OH)/P(VDF-TrFE) composites.

for each alignment state (L, T, and A) have been measured, and the error in the obtained ME coefficient was <5%.

The rotation/deformation of the δ-FeO(OH) nanosheets was determined based on the ME measurements presented above and the theory proposed by Van Den Boomgaard et al.,[26] Zubkov,[27] and Ryu et al.[28] In this way, it is possible to determine the strain derivative, dS/dH, through eq 2,

$$\left(\frac{dS}{dH}\right) = \frac{\alpha}{m_V \times (1 - m_V) \times \left(\frac{d_{33}}{\varepsilon_0 \times \varepsilon} \times \frac{E_Y \times l \times w}{t}\right)_{\text{piezoelectric}}} \tag{2}$$

where m_V, ε_0, ε, E_Y, l, w, and t are the volume fraction of the δ-FeO(OH) nanosheets, the vacuum permittivity, the relative permittivity, the Young's modulus, the length, the width, and the thickness of the composite, respectively.

Assuming that the deformation (λ) generated by the rotation of the δ-FeO(OH) nanosheets increases almost linearly with increasing magnetic field until saturation is reached, λ can be determined by eq 3,

$$\lambda = \left(\frac{dS}{dH}\right) \times B_S \tag{3}$$

where B_S is the magnetic field at which the rotation saturation is achieved.

RESULTS AND DISCUSSION

X-ray diffraction was used for nanosheet characterization (Figure 5a).[29] Figure 5a displays the X-ray patterns of the

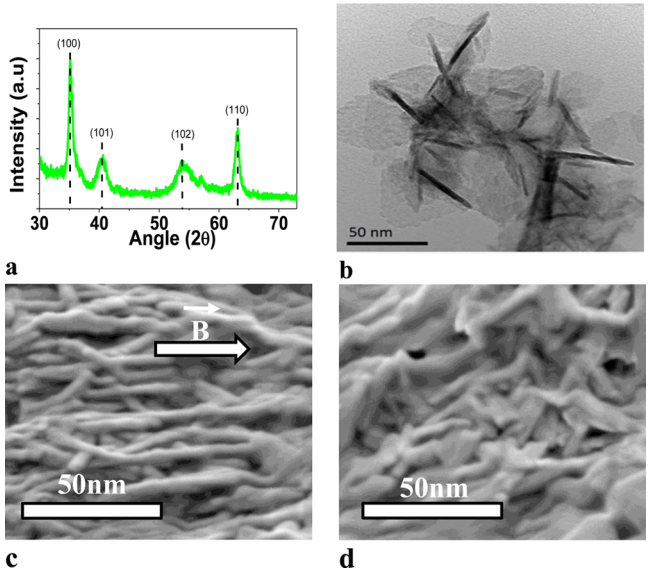

Figure 5. (a) X-ray powder diffraction patterns of feroxyhyte nanosheets; (b) representative TEM images of the nanosheets; (c) L alignment of the δ-FeO(OH) nanosheets within the P(VDF-TrFE) matrix; (d) randomly distributed δ-FeO(OH) nanosheets within the P(VDF-TrFE) matrix.

synthesized nanopowders, showing the typical characteristic structural parameters of the δ-FeO(OH) phase, with reflections corresponding to planes (100), (101), (102), and (110).[30]

The morphology of the produced nanosheets was monitored by TEM, whose images (Figure 5b) revealed an anisotropic sheet structure with dimensions of the order of ~50 nm × 70 nm × 5 nm. Such anisotropy will allow the magnetic alignment of the nanosheets.[31,32] SEM images (Figure 5c, d) reveal the alignment of δ-FeO(OH) within the polymer matrix when the δ-FeO(OH)/ P(VDF-TrFE) composites were prepared under

DOI: 10.1021/acsami.5b01196
ACS Appl. Mater. Interfaces 2015, 7, 11224−11229

a dc magnetic field (Figure 5c) during the material processing. Further, a random nanoparticle distribution is observed in the δ-FeO(OH)/P(VDF-TrFE) composites not submitted to the dc magnetic field during processing, as shown by the random microstructural features of Figure 5d, when compared to the oriented ones in Figure 5c. At lower magnifications the nanoparticles are not observed (and, therefore, the information about nanoparticle orientation) and the same typical morphology of P(VDF-TrFE) processed by solvent evaporation at 80 °C is obtained for all samples.[22] The magnetic behavior of the obtained δ-FeO(OH)/P(VDF-TrFE) composites is represented in Figure 6.

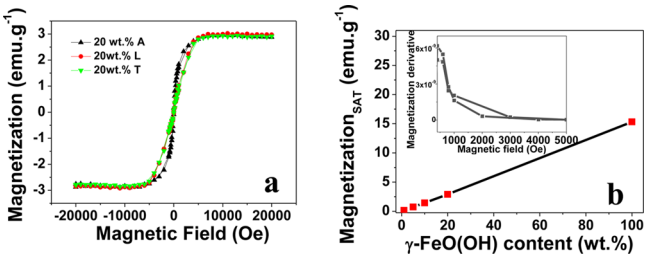

Figure 6. (a) Room-temperature hysteresis loops for the composites with 20 wt % of δ-FeO(OH) with A, L, and T alignments; (b) δ-FeO(OH) wt % dependent saturation magnetization (Magnetization$_{SAT}$). The inset shows the derivative of the magnetization curves of the aligned samples.

The shape and magnetization maximum value (3 emu·g^{-1}, which corresponds to ∼20% of the maximum magnetization of the pure δ-FeO(OH) nanosheets of the hysteresis loops measured in the sample with randomly oriented nanosheets (A samples)) demonstrate that the magnetic response is directly proportional to filler content (Figure 6a). A very small difference is detected between the randomly oriented sample and the oriented samples (L and T), which can be attributed to the magnetization through easy and hard magnetization directions, respectively.[18,19] As expected, for all compositions, the magnetization saturation of the composite increases with increasing δ-FeO(OH) content (Figure 6b). The nanocomposites showing negligible magnetic coercivity and remanence and a magnetization saturating at 8000 Oe.

Because piezoelectricity is a fundamental requirement on ME composites, the piezoelectric responses as a function of the δ-FeO(OH) nanosheets content and over time for the δ-FeO(OH)/P(VDF-TrFE) composites are shown in Figure 7.

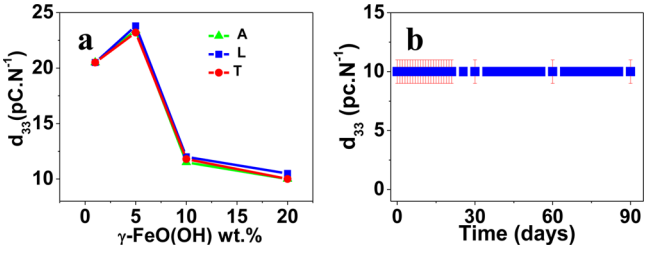

Figure 7. (a) δ-FeO(OH) wt % dependent modulus of piezoelectric constant (d_{33}) for the samples with nanosheets with A, L, and T orientations); (b) modulus of the piezoelectric response over time measured for all the δ-FeO(OH)/P(VDF-TrFE) composites with 20 wt % nanosheets content. It should be noted that the d_{33} value is negative and is given as the modulus in the figures.

Figure 7a reveals first an increase in the piezoelectric response with increasing nanosheets content, as a result of the increased dipolar orientation of the polymer matrix near the interface,[25] due to the strong electrostatic interactions, reaching a maximum value of ∼24 pC·N^{-1} (in modulus) in the sample with 5 wt % of δ-FeO(OH). This effect is related to nanoscale polarization contributions that have been proven to increase the piezoelectric response.[33−36] With increasing filler concentration the piezoelectric response decreases due to an increasingly defective and stiffer polymer matrix.[25,37] Additionally, the piezoelectric response of the polymer matrix is fully dependent on the content of δ-FeO(OH) filler and independent of the filler orientation. Such piezoelectric response is stable over time, until at least 90 days (Figure 7b).

The ME response of the composite with 20 wt % of nanosheets is represented as a function of the intensity of the applied dc magnetic field and the magnetic field direction (Figure 8). Figure 8a shows that the α value increases with the

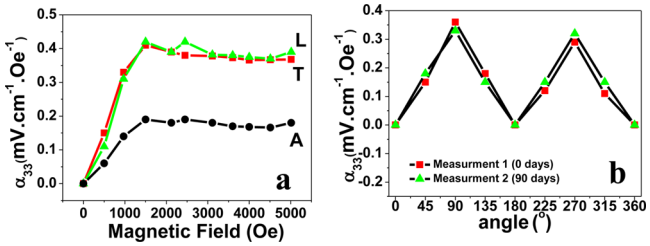

Figure 8. (a) ME response α as a function of the applied magnetic field (parallel to the nanosheet length direction) for the T, L, and A aligned composites, with 20 wt % of nanosheets. (b) ME response α, for the T aligned composite, with 20 wt % of nanosheets, as a function of the angle between the length direction of the δ-FeO(OH) nanosheets and the dc magnetic field direction.

applied dc magnetic field until reaching its maximum value (0.4 mV·cm^{-1}·Oe^{-1}) at ∼1800 Oe, with the α value remaining approximately constant with increasing magnetic field.

The samples with 1, 5, and 10 wt % δ-FeO(OH) content (with A, L, and T alignments) show no ME response, i.e., the response is too small to be observed in the used experimental setup. On composites with 20 wt % δ-FeO(OH), samples with L alignment exhibit similar ME response to the samples with T alignment; on the other hand, samples with no alignment (A samples) show ∼50% lower ME response (Figure 8a).

The highest ME responses were observed when the dc magnetic field was applied perpendicularly to the δ-FeO(OH) length direction alignment (90° and 270°); no ME response was observed when the magnetic field was applied parallel to the alignment (0°, 180°, and 360°), and an intermediate ME response was observed when the magnetic field was applied at angles of 45°, 135°, 225°, and 315° relative to the δ-FeO(OH) alignment (Figure 8b). Those observations are maintained for L aligned samples. The ME response of the samples has been measured to be stable, as the piezoelectric response, up to 90 days, with no relevant variation or aging over time. The ME response angle sensitivity, such as the one represented in Figure 8b, recently proved its applicability on innovative anisotropic magnetic sensors.[16] For practical applications and in order to distinguish, for example, the 45° angle from the 135° one, both with the same ME response, two ME materials, X and Y, should be integrated within the same magnetic sensor with a well-known angle between them, with the comparison of the

DOI: 10.1021/acsami.5b01196
ACS Appl. Mater. Interfaces 2015, 7, 11224−11229

materials response allowing the unambiguous determination of the magnetic field direction.

Such behavior can be related with the impossibility/difficulty of the magnetic moments reorientation and with the anisotropy of the magnetization resulting from the crystallographic restrictions for specific directions.[38] Additionally, it is observed that the ME response saturates at ∼1800 Oe, at the same magnetic field value where the magnetization derivative reaches its minimum (inset of Figure 6b). For higher fields, and contrary to what happens with the usual ME composites (constituted by piezoelectric and magnetostrictive materials),[4,23] the ME response does not decrease, maintaining its maximum value. In this way, increasing the magnetic field from ∼1800 Oe will cause no additional substantial magnetization on δ-FeO(OH) nanosheets,[39] no rotation/movement is promoted, no significant stress is induced on P(VDF-TrFE), and as a consequence no additional ME response is detected. It should be noted that this represents a novel ME response with respect to that previously reported in the literature.

On the basis of eqs 2 and 3, is possible to determine the strain produced by the rotation of the δ-FeO(OH) nanosheets inside the polymer matrix (Table 1).

Table 1. α, m_V, d_{33}, ε, E_Y, l, w, and t values used to determine λ and dS/dH

alignment	α mV·cm^{-1}·Oe^{-1}	m_V	$\lvert d_{33}\rvert$, pC·N^{-1}	ε	E_Y, GPa	$w \times l \times t$, (mm × mm × μm)	$dS/dH \times 10^{-12}$	λ, ppm
L	0.42	0.08	11	12	1.14	6.5 × 12.5 × 50	4.27	0.51
T	0.41						4.17	
A	0.19						1.93	0.23

The results from Table 1 reveal small strains caused by the rotation of the δ-FeO(OH) nanosheets on P(VDF-TrFE) (∼0.2−0.5 ppm) when compared to the typical strains that are transmitted to the piezoelectric polymers by magnetostrictive nanoparticles. Nevertheless, this new ME concept allows the development of polymer-based anisotropic sensors that meet all the most challenging and innovative requirements of the actual magnetic field sensors industry.[4,15−17]

CONCLUSIONS

δ-FeO(OH)/P(VDF-TrFE) magnetoelectic composites have been produced by a simple low-temperature processing method. The nanosheet fillers have been introduced in different filler contents and alignment states (random, transversal, and longitudinal). The piezoelectric response (10−24 pC·N^{-1}), the shape, and the magnetization maximum value (3 emu·g^{-1}) depend on δ-FeO(OH) content. The obtained ME voltage coefficient, with a maximum of ∼0.4 mV·cm^{-1}·Oe^{-1}, depends on filler content and alignment state as well as on both incident magnetic field direction and intensity. Further, a new ME effect is proposed based on the magnetic rotation of the δ-FeO(OH) nanosheets inside the piezoelectric P(VDF-TrFE) polymer matrix. As a conclusion, polymer composites suitable to be used as magnetic field sensors for advanced applications have been developed.

AUTHOR INFORMATION

Corresponding Author

*E-mail: lanceros@fisica.uminho.pt.

Author Contributions

The manuscript was written through contributions of all authors. All authors have given approval to the final version of the manuscript. P.M. and A.L. contributed equally.

Funding

FCT−Portuguese Foundation for Science and Technology.

Notes

The authors declare no competing financial interest.

ACKNOWLEDGMENTS

This work is funded by FEDER funds through the Programa Operacional Factores de Competitividade−COMPETE and by national funds from FCT−Fundação para a Ciência e a Tecnologia, in the framework of the Strategic Project PEST-C/FIS/UI607/2014 and PEST-C/QUI/UI0686/2014. The authors also thank funding from Matepro−Optimizing Materials and Processes, ref NORTE-07-0124-FEDER-000037, cofunded by the Programa Operacional Regional do Norte (ON.2, O Novo Norte), under the Quadro de Referência Estratégico Nacional (QREN), through the Fundo Europeu de Desenvolvimento Regional (FEDER). P.M. and R.G. also acknowledge support from FCT (SFRH/BPD/96227/2013 and SFRH/BD/88397/2012 grants, respectively). V.S. gratefully acknowledges the EU CIG−Marie Curie under the REA grant agreement no. 321642. The microscopy works have been conducted in the Laboratorio de Microscopias Avanzadas at Instituto de Nanociencia de Aragon, Universidad de Zaragoza. V.S. acknowledges the LMA-INA for offering access to their instruments and expertise.

ABBREVIATIONS

ME, Magnetoelectric
P(VDF-TrFE), Poly[vinylidenefluoride-*co*-trifluoroethylene]
PTFE, Polytetrafluoroethylene
TEM, Transmission electron microscopy

REFERENCES

(1) Liu, M.; Howe, B. M.; Grazulis, L.; Mahalingam, K.; Nan, T.; Sun, N. X.; Brown, G. J. Voltage-Impulse-Induced Non-Volatile Ferroelastic Switching of Ferromagnetic Resonance for Reconfigurable Magnetoelectric Microwave Devices. *Adv. Mater.* **2013**, *25*, 4886−4892.

(2) Li, D. Y.; Zeng, Y. J.; Batuk, D.; Pereira, L. M. C.; Ye, Z. Z.; Fleischmann, C.; Menghini, M.; Nikitenko, S.; Hadermann, J.; Temst, K.; Vantomme, A.; Van Bael, M. J.; Locquet, J. P.; Van Haesendonck, C. Relaxor Ferroelectricity and Magnetoelectric Coupling in ZnO−Co Nanocomposite Thin Films: Beyond Multiferroic Composites. *ACS Appl. Mater. Interfaces* **2014**, *6*, 4737−4742.

(3) Kohiki, S.; Okada, K.; Mitome, M.; Kohno, A.; Kinoshita, T.; Iyama, K.; Tsunawaki, F.; Deguchi, H. Magnetic and Magnetoelectric Properties of Self-Assembled $Fe_{2.5}Mn_{0.5}O_4$ Nanocrystals. *ACS Appl. Mater. Interfaces* **2011**, *3*, 3589−3593.

(4) Martins, P.; Lanceros-Méndez, S. Polymer-Based Magnetoelectric Materials. *Adv. Funct. Mater.* **2013**, *23*, 3371−3385.

(5) Silva, M.; Reis, S.; Lehmann, C. S.; Martins, P.; Lanceros-Mendez, S.; Lasheras, A.; Gutiérrez, J.; Barandiarán, J. M. Optimization of the Magnetoelectric Response of Poly(Vinylidene Fluoride)/Epoxy/Vitrovac Laminates. *ACS Appl. Mater. Interfaces* **2013**, *5*, 10912−10919.

(6) Nan, C. W.; Li, M.; Huang, J. H. Calculations of Giant Magnetoelectric Effects in Ferroic Composites of Rare-Earth−Iron Alloys and Ferroelectric Polymers. *Phys. Rev. B* **2001**, *63*, 144415.

(7) Jin, J.; Zhao, F.; Han, K.; Haque, M. A.; Dong, L.; Wang, Q. Multiferroic Polymer Laminate Composites Exhibiting High Magnetoelectric Response Induced by Hydrogen-Bonding Interactions. *Adv. Funct. Mater.* **2014**, *24*, 1067−1073.

DOI: 10.1021/acsami.5b01196
ACS Appl. Mater. Interfaces 2015, 7, 11224−11229

(8) Rani, R.; Juneja, J. K.; Singh, S.; Raina, K. K.; Prakash, C. Multiferroic Properties of 0.05 NZF − 0.95 $Ba_{0.9-3x/2}Sr_{0.1}La_xTiO_3$ Magnetoelectric Composites. *Adv. Mater. Lett.* **2014**, *5*, 229−233.
(9) Krawczyk, M.; Grundler, D. Review and Prospects of Magnonic Crystals and Devices with Reprogrammable Band Structure. *J. Phys.: Condens. Matter* **2014**, *26*, 123202.
(10) Hu, J. M.; Shu, L.; Li, Z.; Gao, Y.; Shen, Y.; Lin, Y. H.; Chen, L. Q.; Nan, C. W. Film Size-Dependent Voltage-Modulated Magnetism in Multiferroic Heterostructures. *Philos. Trans. R. Soc., A* **2014**, *372*, 0444.
(11) Zhang, J.; Li, P.; Wen, Y.; He, W.; Yang, A.; Lu, C.; Qiu, J.; Wen, J.; Yang, J.; Zhu, Y.; Yu, M. High-Resolution Current Sensor Utilizing Nanocrystalline Alloy and Magnetoelectric Laminate Composite. *Rev. Sci. Instrum.* **2012**, *83*, 115001.
(12) Shi, Z.; Nan, C.-W.; Zhang, J.; Ma, J.; Li, J.-F. Magnetoelectric Properties of Multiferroic Composites with Pseudo-1−3-Type Structure. *J. Appl. Phys.* **2006**, *99*, 124108.
(13) Yuse, K.; Guiffard, B.; Belouadah, R.; Petit, L.; Seveyrat, L.; Guyomar, D. Polymer Nanocomposites for Microactuation and Magneto-Electric Transduction Front. *China Mech. Eng.* **2009**, *4*, 350−354.
(14) Martins, P.; Lopes, A. C.; Lanceros-Mendez, S. Electroactive Phases of Poly(Vinylidene Fluoride): Determination, Processing and Applications. *Prog. Polym. Sci.* **2013**, *39*, 683−706.
(15) Lee, D. G.; Kim, S. M.; Yoo, Y. K.; Han, J. H.; Chun, D. W.; Kim, Y. C.; Kim, J.; Hwang, K. S.; Kim, T. S.; Jo, W. W.; Kim, H.; Song, S. H.; Lee, J. H. Ultra-Sensitive Magnetoelectric Microcantilever at a Low Frequency. *Appl. Phys. Lett.* **2012**, *101*, 182902.
(16) Chen, S.; Yang, X.; Ouyang, J.; Lin, G.; Jin, F.; Tong, B. Fabrication and Characterization of Shape Anisotropy AlN/FeCoSiB Magnetoelectric Composite Films. *Ceram. Int.* **2014**, *40*, 3419−3423.
(17) Liu, M.; Li, S.; Obi, O.; Lou, J.; Rand, S.; Sun, N. X. Electric Field Modulation of Magnetoresistance in Multiferroic Heterostructures for Ultralow Power Electronics. *Appl. Phys. Lett.* **2011**, *98*, 222509.
(18) Lin, W.; Miao, Y.; Zhang, H.; Liu, B.; Liu, Y.; Song, B.; Wu, J. Two-Dimensional Magnetic Field Vector Sensor Based on Tilted Fiber Bragg Grating and Magnetic Fluid. *J. Lightwave Technol.* **2013**, *31*, 2599−2605.
(19) Oh, Y. S.; Crane, S.; Zheng, H.; Chu, Y. H.; Ramesh, R.; Kim, K. H. Quantitative Determination of Anisotropic Magnetoelectric Coupling in $BiFeO_3$−$CoFe_2O_4$ Nanostructures. *Appl. Phys. Lett.* **2010**, *97*, 052902.
(20) Ettelt, D.; Rey, P.; Jourdan, G.; Walther, A.; Robert, P.; Delamare, J. 3D Magnetic Field Sensor Concept for Use in Inertial Measurement Units (IMUs). *J. Microelectromech. Syst.* **2014**, *23*, 324−333.
(21) Liu, R.; Zhang, M.; Niu, E.; Li, Z.; Zheng, X.; Wu, R.; Zuo, W.; Shen, B.; Hu, F.; Sun, J. Structure and Magnetic Properties of Low-Temperature Phase Mn-Bi Nanosheets with Ultra-High Coercivity and Significant Anisotropy. *J. Appl. Phys.* **2014**, *115*, 17A742.
(22) California, A.; Cardoso, V. F.; Costa, C. M.; Sencadas, V.; Botelho, G.; Gómez-Ribelles, J. L.; Lanceros-Mendez, S. Tailoring Porous Structure of Ferroelectric Poly(Vinylidene Fluoride-Trifluoroethylene) by Controlling Solvent/Polymer Ratio and Solvent Evaporation Rate. *Eur. Polym. J.* **2011**, *47*, 2442−2450.
(23) Martins, P.; Lasheras, A.; Gutierrez, J.; Barandiaran, J. M.; Orue, I.; Lanceros-Mendez, S. Optimizing Piezoelectric and Magnetoelectric Responses on $CoFe_2O_4$/P(Vdf-Trfe) Nanocomposites. *J. Phys. D: Appl. Phys.* **2011**, *44*, 495303.
(24) Israel, C.; Petrov, V. M.; Srinivasan, G.; Mathur, N. D. Magnetically Tuned Mechanical Resonances in Magnetoelectric Multilayer Capacitors. *Appl. Phys. Lett.* **2009**, *95*, 072505.
(25) Martins, P.; Moya, X.; Phillips, L. C.; Kar-Narayan, S.; Mathur, N. D.; Lanceros-Mendez, S. Linear Anhysteretic Direct Magnetoelectric Effect in $Ni_{0.5}Zn_{0.5}Fe_2O_4$/Poly(Vinylidene Fluoride-Trifluoroethylene) 0−3 Nanocomposites. *J. Phys. D: Appl. Phys.* **2011**, *44*, 482001.
(26) Van Den Boomgaard, J.; Van Run, A. M. J. G.; Van Suchtelen, J. Magnetoelectricity in Piezoelectric-Magnetostrictive Composites. *Ferroelectrics* **1975**, *10*, 295−298.
(27) Zubkov, A. S. Impulsive Piezoceramic Generators with Magnetostrictive Drive. *Electr. Technol. USSR* **1978**, *00134155*, 59−78.
(28) Ryu, J.; Priya, S.; Uchino, K.; Kim, H. E. Magnetoelectric Effect in Composites of Magnetostrictive and Piezoelectric Materials. *J. Electroceram.* **2002**, *8*, 107−119.
(29) Tan, Y.; Sun, D.; Yu, H.; Yang, B.; Gong, Y.; Yan, S.; Chen, Z.; Cai, Q.; Wu, Z. Crystallization Mechanism Analysis of Noncrystalline Ni-P Nanoparticles through XRD, HRTEM and XAFS. *CrystEngComm* **2014**, *16*, 9657−9668.
(30) Chagas, P.; Da Silva, A. C.; Passamani, E. C.; Ardisson, J. D.; De Oliveira, L. C. A.; Fabris, J. D.; Paniago, R. M.; Monteiro, D. S.; Pereira, M. C. δ-FeOOH: A Superparamagnetic Material for Controlled Heat Release under AC Magnetic Field. *J. Nanopart. Res.* **2013**, *15*, 1544.
(31) Ten, E.; Jiang, L.; Wolcott, M. P. Strategies for Preparation of Oriented Cellulose Nanowhiskers Composites. *ACS Symp. Ser.* **2012**, *1107*, 17−36.
(32) Gu, Y.; Kornev, K. G. Alignment of Magnetic Nanorods in Solidifying Films. *Part. Part. Syst. Charact.* **2013**, *30*, 958−963.
(33) Chu, B.; Lin, M.; Neese, B.; Zhou, X.; Chen, Q.; Zhang, Q. M. Large Enhancement in Polarization Response and Energy Density of Poly(Vinylidene Fluoride-Trifluoroethylene-Chlorofluoroethylene) by Interface Effect in Nanocomposites. *Appl. Phys. Lett.* **2007**, *91*, 831−838.
(34) Guo, D.; Zeng, F.; Dkhil, B. Ferroelectric Polymer Nanostructures: Fabrication, Structural Characteristics and Performance under Confinement. *J. Nanosci. Nanotechnol.* **2014**, *14*, 2086−2100.
(35) Guo, D.; Setter, N. Impact of Confinement-Induced Cooperative Molecular Orientation Change on the Ferroelectric Size Effect in Ultrathin P(VDF-TrFE) Films. *Macromolecules* **2013**, *46*, 1883−1889.
(36) Guo, D.; Stolichnov, I.; Setter, N. Thermally Induced Cooperative Molecular Reorientation and Nanoscale Polarization Switching Behaviors of Ultrathin Poly(Vinylidene Fluoride-Trifluoroethylene) Films. *J. Phys. Chem. B* **2011**, *115*, 13455−13466.
(37) Li, J.; Seok, S. I.; Chu, B.; Dogan, F.; Zhang, Q.; Wang, Q. Nanocomposites of Ferroelectric Polymers with TiO_2 Nanoparticles Exhibiting Significantly Enhanced Electrical Energy Density. *Adv. Mater.* **2009**, *21*, 217−221.
(38) Aida, T.; Kawai, T.; Ohtake, M.; Futamoto, M.; Inaba, N. Relationship between Magnetostriction and Magnetic Domain Structure in Fe-Based Alloy Single-Crystal Films with Bcc(001) Orientation. *IEEE Trans. Magn.* **2014**, *50*, 1−4.
(39) Yuan, J.; Gao, H.; Schacher, F.; Xu, Y.; Richter, R.; Tremel, W.; Müller, A. H. E. Alignment of Tellurium Nanorods Via a Magnetization−Alignment−Demagnetization ("MAD") Process Assisted by an External Magnetic Field. *ACS Nano* **2009**, *3*, 1441−1450.

DOI: 10.1021/acsami.5b01196
ACS Appl. Mater. Interfaces 2015, 7, 11224−11229